Genes & Diseases (2022) 9, 1074–1085

Available online at www.sciencedirect.com

ScienceDirect

journal homepage: http://ees.elsevier.com/gendis/default.asp

FULL LENGTH ARTICLE

AAV6 as an effective gene delivery vector for prolonged transgene expression in intervertebral disc cells *in vivo*

Chi Heon Kim [a,b], Colleen Oliver [a,b], Hamid Dar [a], Hicham Drissi [a,b,], Steven M. Presciutti [a,b,*]**

[a] *Department of Orthopaedics, Emory University School of Medicine, Atlanta, GA 30329, USA*
[b] *Atlanta Veteran Affairs Medical Center, Decatur, GA 30030, USA*

Received 11 July 2020; received in revised form 7 December 2020; accepted 22 December 2020
Available online 30 December 2020

KEYWORDS
Adeno-associated virus;
Bioluminescence imaging;
Cell permeabilization peptide;
Intervertebral disc;
Lightsheet microscopy;
Nucleus pulposus transduction;
Tissue clearing

Abstract Intervertebral disc degeneration is the main contributor to low back pain, now the leading cause of disability worldwide. Gene transfer, either in a therapeutic attempt or in basic research to understand the mechanisms of disc degeneration, is a fascinating and promising tool to manipulate the complex physiology of the disc. Viral vectors based on the adeno-associated virus (AAV) have emerged as powerful transgene delivery vehicles yet a systematic investigation into their respective tropism, transduction efficiency, and relative toxicity have not yet been performed in the disc *in vivo*. Herein, we used *in vivo* bioluminescence imaging to systematically compare multiple AAV serotypes, injection volumes, titers, promoters, and luciferase reporters to determine which result in high transduction efficiency of murine nucleus pulposus (NP) cells *in vivo*. We find that AAV6 using a CAG promoter to drive transgene expression, delivered into the NP of murine caudal discs at a titer of 10^{11} GC/mL, provides excellent transduction efficiency/kinetics and low toxicity *in vivo*. We also show, for the first time, that the transduction of NP cells can be significantly boosted *in vivo* by the use of small cell permeabilization peptides. Finally, to our knowledge, we are the first to demonstrate the use of optical tissue clearing and three-dimensional lightsheet microscopy in the disc, which was used to visualize fine details of tissue and cell architecture in whole intact discs following AAV6 delivery. Taken together, these data will contribute to the success of using AAV-mediated gene delivery for basic and translational studies of the IVD.

* Corresponding author. Emory Orthopaedics and Spine Center, 59 Executive Park S NE, Atlanta, GA 30329, USA.
** Corresponding author. Emory Orthopaedics and Spine Center, 59 Executive Park S NE, Atlanta, GA 30329, USA.
E-mail addresses: hicham.drissi@emory.edu (H. Drissi), steven.presciutti@emory.edu (S.M. Presciutti).
Peer review under responsibility of Chongqing Medical University.

https://doi.org/10.1016/j.gendis.2020.12.009

Introduction

Low back pain (LBP) is now the leading cause of disability worldwide, affecting approximately 637 million individuals worldwide.[1] Intervertebral disc (IVD) degeneration (IDD) is the major contributor to LBP and is the pathologic foundation for almost all degenerative disorders of the spine.[2] IDD remains a crippling clinical problem that affects the global population both physically and socioeconomically, with the United States alone spending an estimated $200 billion annually to treat IDD and its associated disabilities.[3] Despite the scope and magnitude of the problem, a successful clinical treatment for IDD does not currently exist. Accordingly, there is an urgent need for effective IDD treatments that address the underlying pathophysiology of the disease early, rather than address only end-stage symptoms such as LBP.

From a biochemical standpoint, the balance between the synthesis and degradation of collagen and proteoglycans by the annulus fibrosus (AF) and the nucleus pulposus (NP) is critical in maintaining the integrity and functionality of the disc. To treat the negative imbalance between catabolism and anabolism in IDD, a variety of biological approaches, including growth factor injection and cell and gene therapy, has received considerable attention over the past 20 years due to the limitations of currently available treatments.[4] Recent studies on the mechanisms that underlie the development of IDD have created a base of physiological and genetic information that have identified multiple potential points of intervention for treatment.[5–7] On the basis of these insights, gene therapy for IDD has shown early success, both *in vitro* and *in vivo*, by producing gene products that either block catabolism and inflammation or enhance anabolism in the NP of the IVD.[8–13] Moreover, gene therapy remains an exciting and viable option to treat a chronic disease like IDD because it can afford a sustained biological effect with a single injection as opposed to growth factor or cell-based treatments that require multiple repeated injections. In addition to clinical treatment, the use of virus-based gene manipulation can be a robust tool to help dissect basic fundamental questions regarding disc homeostasis and disease progression.[7]

While gene therapy remains a viable treatment strategy for IDD, the majority of the studies to-date have used either lentiviral or adenoviral gene delivery systems. Critical concerns over the use of these delivery systems in clinical applications remain, however, due to random gene incorporation and immune reactions.[14–21] An alternative gene delivery strategy is the adeno-associated virus (AAV) system, which is stable, less immunogenic, and because it does not express any viral gene, remains the only virus that has not been conclusively shown to be etiologic in any human disease to-date.[22] As such, recombinant (r)AAV vectors have been used for gene therapy to treat several human diseases in a number of Phase I/II clinical trials,[23–31] and more recently have shown promising initial results in the retardation or reversal of IDD progression.[12,13,32] In addition, AAV permits prolonged transgene expression of therapeutic genes and has high transduction efficiency in both dividing and non-dividing cells,[33,34] making it a good candidate for gene therapy in the IVD due to the very low baseline levels of mitosis[35] and high levels of senescence[36–38] present even in healthy, non-degenerated NP cells.

One critical factor determining transduction efficiency (how effective a potential gene therapy treatment is going to be relative to the initial viral dose given) is the cellular tropism of different AAV serotypes.[39,40] Specific to cells of the IVD, it has been previously shown that AAV serotypes-2 and -6 provide the best tropism in human NP cells *in vitro*, while other serotypes had poorer transduction efficiency and provided little to no transgene expression.[41] To our knowledge, however, the transduction efficiency of different AAV serotypes in NP cells has not been determined *in vivo*. Also, it remains unknown what viral titer and injection volume produce good transduction efficiency when injected into murine IVDs, which is important because murine IVD models are widely used and considered a gold standard for the study of transgenic animals. Herein, we systematically assessed the transduction efficiency of murine NP cells in caudal IVDs *in vivo* using AAV-2 and -6 serotypes, injection volumes, viral titers, and gene promoters. The kinetics of transgene expression in the IVD was determined by temporally measuring the intensity of *in vivo* bioluminescence following local injection of AAV-fLuc (firefly luciferase) directly into the NP of murine caudal IVDs. Finally, we assessed the ability of a synthetic cell-permeable peptide (CPP) to further increase transduction efficiency, which has never been assessed in the disc, by performing novel three-dimensional (3D) imaging of the IVD using optical tissue clearing and light sheet microscopy (to our knowledge, a first in the IVD field). This 3D imaging also allowed for assessment of the tissue architecture of the NP and whole disc 4 weeks following local delivery of AAV ± CPP to assess for evidence of any toxicity or pathologic phenotypes in the IVD.

This is the first study to evaluate how different AAV serotypes, gene promoters, CPPs, and other factors affect the transduction efficiency of IVD cells *in vivo*. These findings will contribute to the success of using AAV-mediated gene delivery in a variety of applications for basic and translational studies of the IVD, as well as potentially aid in the design of more efficient and effective gene therapeutic approaches for the treatment of IDD.

Materials and methods

All the experiments involving animals were conducted in accordance with the National Institutes of Health *Guide for the Care and Use of Laboratory Animals* and were approved by the Institutional Animal Care and Use Committee of the Atlanta VAMC (#2017—100794). Male and female C57Bl/6 mice were purchased from Jackson Laboratories (Wilmington, MA), while male and female mTmG mice (Stock# 007676) were acquired from Jackson Laboratories (Bar Harbor, ME).

Transduction of murine caudal IVDs *in vivo*

The AAV-2 and -6 serotypes used for fLuc-based bioluminescence, all with either the CAG (combination of a cytomegalovirus early enhancer element, the promoter of chicken beta-actin gene, and a splice acceptor of rabbit beta-globin

gene) or EF1-α (human eukaryotic translation elongation factor 1 alpha) promoter, were custom synthesized from Vector Biolabs (Fig. 1). AAV-2 and -6 for gLuc-based bioluminescence (AAV-CAG-gLuc) was custom synthesized from GeneCopoeia (Rockville, MD) (not shown). For tissue clearing and 3D lightsheet microscopy, AAV6-CMV-Cre were custom synthesized by SignaGen (Rockville, MD). The CPP, LAH4 (sequence: KKALLALALHHLAHLALHLALALKKAC), was custom synthesized from GenScript (Piscataway, NJ).

At 8–10 weeks of age, either C57Bl/6 or mTmG mice were anesthetized with 2% isoflurane and oxygen. The Co6/7 (caudal tail disc 6/7) disc was identified by palpation and confirmed using fluoroscopic imaging (Fig. S1). When CPP was used in conjunction with AAV, the virus was pre-incubated with CPP (final concentration: 100 μmol/L) in PBS for 30 min at 37 °C. In all cases, after cleaning the tail with alcohol, a 33G Hamilton (Reno, NV) Neuros® syringe was used to puncture the AF unilaterally and fluoroscopy was used to confirm that the tip of the needle was in the middle of the NP compartment. An injection of 3–5 μL containing variable concentrations of AAV (10^6, 10^9 and 10^{12} GC/mL), with or without the addition of CPP, was then slowly injected into the disc ($n = 3$, each group). After leaving the needle in place for 5 s, the needle was carefully removed without excessive mechanical disruption of the NP and AF. All mice were then allowed to recover in isolation prior to being placed back into their cage with other animals. All mice were allowed to feed and have activity *ad libitum* and were monitored closely for loss of mobility or any interruption in normal grooming activity.

Bioluminescence imaging of IVDs

The mice were again anesthetized with 2% isoflurane and oxygen. In experiments in which AAV-fLuc was used, the d-luciferin substrate (Biotium, Hayward, CA) was injected intraperitoneally at a dose of 150 μg/g of body weight. In contrast, when AAV-gLuc was used, either 100 μg of standard coelenterazine or 100 μg of coelenterazine-SOL (Nanolight, Pinetop, AZ) was injected intraperitoneally. The mice were then placed in a dark chamber inside of a Bruker In Vivo Xtreme system (Billerica, Massachusetts). Images were generated using a cryogenically cooled charge-coupling device camera IVIS 100 (Xenogen, Alameda, CA). For each mouse, bioluminescence images were taken at either 20 min (fLuc) or 1 min (gLuc) following substrate injection. Both light and dark images of mice were collected, and the dark images were then pseudo-colored using the Bruker software (Molecular Imaging software v7.5). Visual output was set to represent the number of photons emitted/second/cm^2 as a false color image, where maximum intensity is colored white and the minimum is colored violet. All animals were imaged on a schedule of 3, 7, 14, 21, 28, 35, 42, and 56 days following injection of AAV into the caudal IVD.

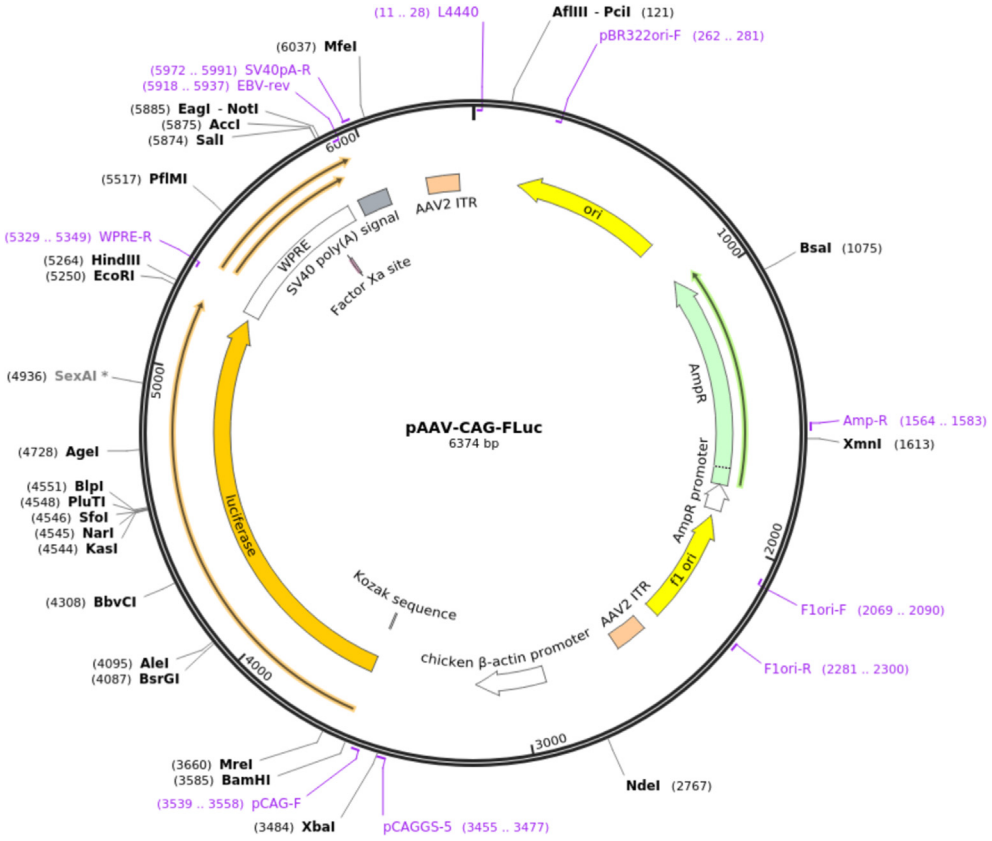

Figure 1 The AAV-2 and -6 serotypes used for fLuc-based bioluminescence used either the CAG (combination of a cytomegalovirus early enhancer element, the promoter of chicken beta-actin gene, and a splice acceptor of rabbit beta-globin gene) or EF1-α (human eukaryotic translation elongation factor 1 alpha) promoter. These custom designed adenoviral vectors were synthesized from Vector Biolabs (Malvern, PA).

Quantification of luciferase expression *in vivo*

At each of the assessed time-points, a defined region of interest (1.5 mm diameter area that included the peak photon count) was designated surrounding each of the injected caudal disc segments using the Bruker Molecular Imaging software v7.5 in order to quantify the total flux (photons/sec/cm^2/radian), or luciferase activity, being released following injection of either d-luciferin (fLuc) or coelenterazine (gLuc). For each condition tested, the mean flux was determined for all animals at each time-point ($n = 3$).

Tissue clearing of IVDs

In short, each mouse was anesthetized with 5% isoflurane and oxygen and placed on the operating table on its back on a warm circulating water pad. After confirming adequate anesthesia, an incision was made with the scalpel through the abdomen equivalent to the length of the diaphragm. With sharp scissors, the connective tissue at the bottom of diaphragm was cut to allow access to rib cage. With large scissors ribs just to the left of the midline were cut and two horizontal cuts were made through the rib cage to open the thoracic cavity and expose the heart. While holding beating heart steady with forceps, a needle was inserted directly into the left ventricle. The needle position was secured by clamping in place near the point of entry. The infusion of 0.1 M phosphate buffered solution (PBS) that is heparinized (10 U/mL) was then run for 5–10 min at a flow rate of 20–30 mL/min (VWR 23609-170). After the blood was cleared from the body, the infusing solution was changed to 4% paraformaldehyde (PFA). Perfusion was determined complete when reflex spontaneous movement was observed and the liver exhibited pallor.

At this point, the caudal spine was carefully dissected out of the body. The PEGASOS method[42] of optically clearing tissue was used in all animals in which 3D lightsheet microscopy was to be performed. To start, each of the dissected spines was post-fixed in 4% PFA for 1–2 d at 4 °C. Next, fixed samples were decalcified with 0.5 M EDTA in a 37 °C shaker (~100 rpm) for 2–4 d with daily medium change. Following that, samples were decolorized by placement into 25% Quadrol (Sigma–Aldrich, St. Louis, MO) for 1–2 days at 37 °C under constant shaking (~100 rpm) with daily medium change. Samples were then immersed in gradient delipidation solutions (tert-Butanol + Quadrol) for 2 days in a 37 °C shaker, followed by dehydration solution treatment for 2 days and BB-PEG clearing medium treatment ([75% v/v Benzyl Benzoate + 25% v/v PEG-MMA-500] + 3% w/v Quadrol) for at least 1 day until reaching transparency.

Three-dimensional lightsheet microscopy

To image the cleared intervertebral disc segment specimens, a LaVision Biotec UltraMicroscope II (Bielefeld, Germany) equipped with an sCMOS camera (Andor Neo), a 2 Å~/0.5 objective lens equipped with a dipping cap, and an Olympus MV×10 zoom microscope body (magnification range of Å~0.63 to Å~6.3) was used. The cleared tissues were mounted on the sample holder and incubated with the final clearing solution in the sample reservoir. A tiling lightsheet tiled at multiple positions within the field of view was used to illuminate the sample, and the sample was scanned with a 3.2 × /0.25NA objective axially at a ~2 μm step size to image the selected region of interests in 3D. Imaging processing and 3D rendering was performed on a Dell Precision T7600 workstation with dual Xeon 2670 processor, 128 GB RAM, and AMD Radeon 480 graphic card.

All raw image data were collected in a lossless 16-bit TIFF format. Blind deconvolution processing was performed using Autoquant X3 (Media Cybernetics, Rockville, Maryland). Tiling of multiple image stacks were performed using Image J (NIH).[43] 3D reconstruction images and movies were generated using Imaris v.9.5 (Bitplane, Zürich, Switzerland). Stack images were generated using the "volume rendering" function and optical slices were obtained using the "orthoslicer" function. 3D pictures were generated to calculate the number of transduced NP cells using the "snapshot" function, which was calculated by dividing the number of GFP + cells (indicating successful Cre recombination via AAV transduction) by total number of NP cells.

Statistics and calculations

For statistical analysis, the data were evaluated for significance by performing a one-way analysis of variance (ANOVA) with Bonferroni Post Hoc test (equal variances assumed) or Dunnett's T3 Post Hoc test (equal variances not assumed) using Statistical Products for Social Sciences Version 16.0 (SPSS 16.0) for Windows (SPSS, Chicago, IL). Interobserver agreement for IDD grading of lightsheet images was calculated by using Fleiss' Kappa.[44] Probability values of $P < 0.05$ were considered to be statistically significant. Data are expressed as means ± standard error of the mean (SEM).

Results

AAV titer and injection volume for murine IVDs

We first determined the kinetics for *in vivo* bioluminescence using a fLuc reporter in a murine IVD, which to our knowledge has not been previously reported. AAV6 particles were chosen to deliver the fLuc reporter because this serotype has previously been shown to show strong tropism for NP cells *in vitro*[41] and expression was driven by the cytomegalovirus early enhancer/chicken β-actin, or CAG, promoter. Seven days following local delivery of AAV6-CAG-fLuc particles, an IP injection of D-luciferase was administered into C57Bl/6 mice ($n = 10$). Whole-body *in vivo* bioluminescence imaging (BLi) was then acquired at 5, 10, 15, 20, 25, and 30 min post-injection to determine how long it would take the substrate to diffuse from the peritoneal cavity, enter systemic the vasculature system, diffuse across the cartilaginous endplates of caudal IVDs, and interact with the fLuc protein now being expressed in the NP cells. It was found that 20 min provided an optimal time to perform BLi in this setting, as this time point provided a good balance between near maximal intensity, decreased variability between animals, and efficient time from substrate injection to image acquisition (Fig. 2A). Therefore, a

time period of 20 min between administration of d-luciferin and BLi was used in all subsequent experiments reported hereafter.

Next, we wanted to determine the appropriate volume of AAV to deliver locally into murine caudal IVD, which is a simple but currently undefined experimental variable in the literature. We therefore injected Co6/7 (caudal disc # 6/7) with AAV6-CAG-fLuc at a titer of 10^{11} GC (genome copies) per mL using a 33G needle and an injection volume of either 3 or 5 μL ($n = 6$ each). A volume of 5 μL was chosen because it is the most commonly reported in the literature for murine caudal IVD injections.[45] Likewise, the titer of 10^{11} GC/mL was chosen here based off of previous reports.[45] Of note, one of the first things we noticed when performing the injections in the 5 μL group was that a subtle loss of resistance was noted on the plunger of the syringe in >80% of the animals after about 4 μL were injected, possibly indicating loss of annular integrity from the volume being injected. This was not appreciated in the mice receiving an injection volume of 3 μL. There were no adverse signs visually apparent and no signs of pain or distress in any of the animals following injection, however. BLi was then performed 3, 7, 14, 21, 28, 42, and 56 days following local delivery of AAV into the disc. At all timepoints, a 3 μL injection volume provided superior BLi intensity and better kinetics compared to the animals receiving 5 μL (Fig. 2B). In addition, all mice that received a volume of 5 μL had their BLi intensity eccentrically placed to the side of the disc in which the injection was performed, whereas all of the mice who received an injection volume of 3 μL had their bioluminescence centered directly in the center (NP) of the injected disc (Fig. 2C, D). This further suggests that even the larger, more proximal caudal IVDs, such as Co6/7, cannot tolerate an injection volume of 5 μL because it mechanically disrupts the integrity of the AF. Therefore, an injection volume of 3 μL was used in all subsequent experiments.

Additionally, we sought to determine how the titer of delivered AAV particles would affect the transduction efficiency and the kinetics of transgene expression in murine caudal IVDs *in vivo*. Mice received a local injection (3 μL) of AAV6-CAG-fLuc particles into their Co6/7 disc at a titer of either 10^6, 10^9, or 10^{11} GC/mL. BLi was then performed at 3, 7, 14, 21, 28, 35, 42, and 56 days following injection of AAV6-fLuc to determine the transduction efficiency and kinetics for each titer *in vivo*. The titer of 10^6 GC/mL produced no BLi signal at any of the timepoints tested, while a titer of 10^{11} was found to provide superior results

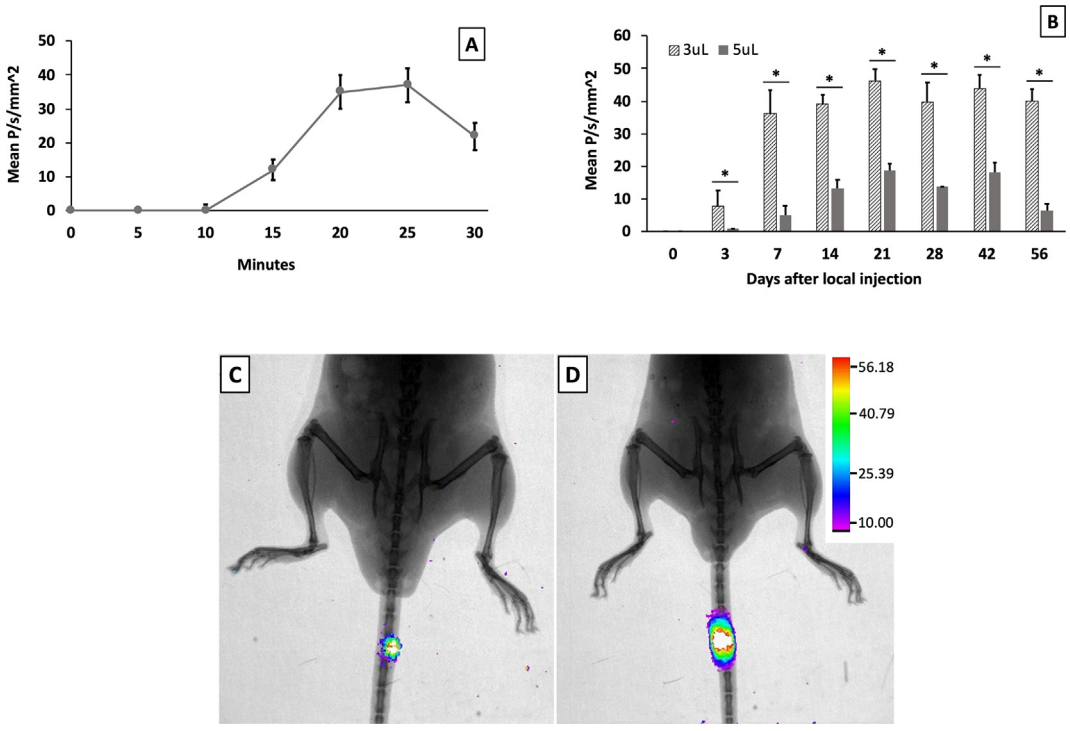

Figure 2 Kinetics of firefly luciferase-based bioluminescence in NP cells in vivo. Seven days following local delivery of AAV6-CAG-fLuc particles, an IP injection of D-luciferase was administered into C57Bl/6 mice (n Z 10). Whole-body *in vivo* bioluminescence imaging (BLi) was then acquired serially. It was found that 20 min provided an optimal time to perform BLi in this setting, providing a good balance between near maximal intensity and efficient time from substrate injection to image acquisition. Injection volume of AAV particles affects transduction efficiency and kinetics. AAV6-CAG-fLuc was injected into Co6/7 at a titer of 10^{11} GC (genome copies) per mL using a 33G needle and an injection volume of either 3 or 5 μL ($n = 6$ each). BLi was then performed serially. At all timepoints, a 3 μL injection volume provided superior BLi intensity and better kinetics compared to the animals receiving 5 μL (**A**). Furthermore, all mice that received a volume of 5 μL had their BLi intensity eccentric to the injected disc (**B**), suggesting that this volume mechanically disrupts the integrity of the AF. In contrast, all of the mice who received a 3 μL injection showed maximum BLi from the center of the injected disc. Error bars show SEM. '*' represents statistical significance, $P < 0.05$. P = photon, s = seconds.

compared to 10^9 (Fig. 3). The mean peak intensity on BLi of AAV6 was 52 P/s/mm^2 and occurred earlier at 21 days, compared to the mean peak intensity on AAV2 (16 P/s/mm^2, $P < 0.05$), which occurred later at 6 weeks (Fig. 3A). Representative BLi pictures for the 10^9 and 10^{11} titers (42-day timepoint) are shown in Figure 3B and C, respectively. Taken together, a titer of 10^{11} GC/mL was used in all subsequent experiments.

Comparison of AAV serotypes

It has previously been found that AAV2 and AAV6 have the highest tropism for NP cells compared to other AAV serotypes *in vitro*.[41] To determine their effectiveness for *in vivo* applications, we injected each of these serotypes (3 μL, 10^{11} GC/mL) into caudal IVDs (Co6/7) of C57Bl/6 mice and performed longitudinal BLi at 3, 7, 14, 21, 28, 35, 42, and 56 days to determine the relative transduction efficiency and kinetics for each serotype. As shown in Figure 4A, AAV6 showed better transduction efficiency (greatest bioluminescence intensity, 46.2 P/s/mm^2) and kinetics (earliest signal after injection and quickest rise to maximal intensity) compared to AAV2. Moreover, AAV6 hit near maximal BLi intensity 7 days following local injection into the NP (46.19 P/s/mm^2) and was able to maintain a similar amount of fLuc expression up to 56 days, while AAV2 took at least twice as long to reach maximal intensity. Mean peak intensity with AAV2 was also significantly less than what was achieved with AAV6 (22.34 P/s/mm^2, $P < 0.05$). This demonstrates that, similar to what was reported by Mern and colleagues *in vitro*,[41] AAV6 provides a relatively high amount of tropism for NP cells *in vivo*. Because of the high transduction efficiency and favorable kinetics, AAV6 was chosen for all subsequent experiments conducted hereafter.

Comparison of gene promoters

Previous studies have demonstrated that, in a variety of settings, different constitutive promoters used in AAV vectors can demonstrate variable kinetics with respect to transgene expression that is tissue specific. For example,

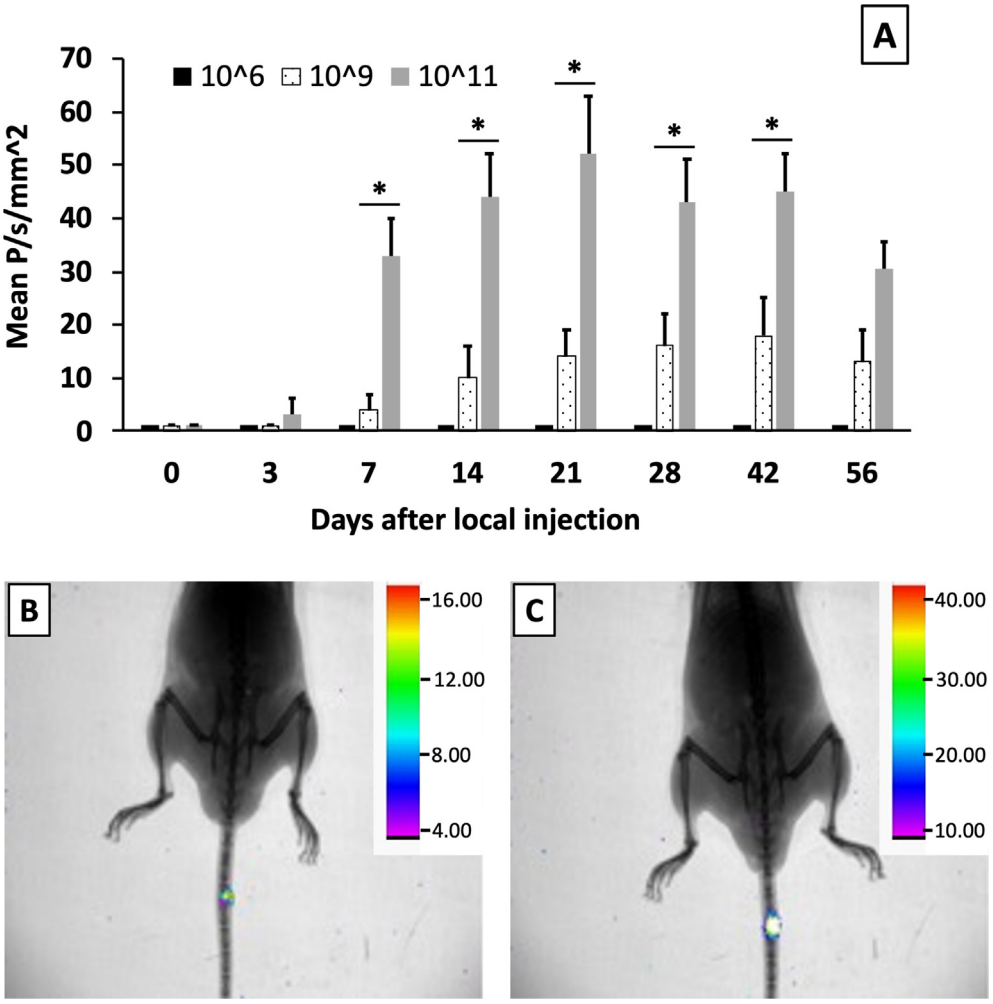

Figure 3 Viral titer affects transduction efficiency and kinetics. Mice received a 3 μL local injection of AAV6-CAG-fLuc particles into their Co6/7 disc at a titer of either 10^6, 10^9, or 10^{11} GC/mL. BLi was then performed serially to determine the transduction efficiency and kinetics for each titer *in vivo* (**A**). Representative BLi pictures for the 10^9 and 10^{11} titers (42-day timepoint) are also shown in **B** and **C**, respectively. Error bars show SEM. '*' represents statistical significance, $P < 0.05$. P = photon, s = seconds.

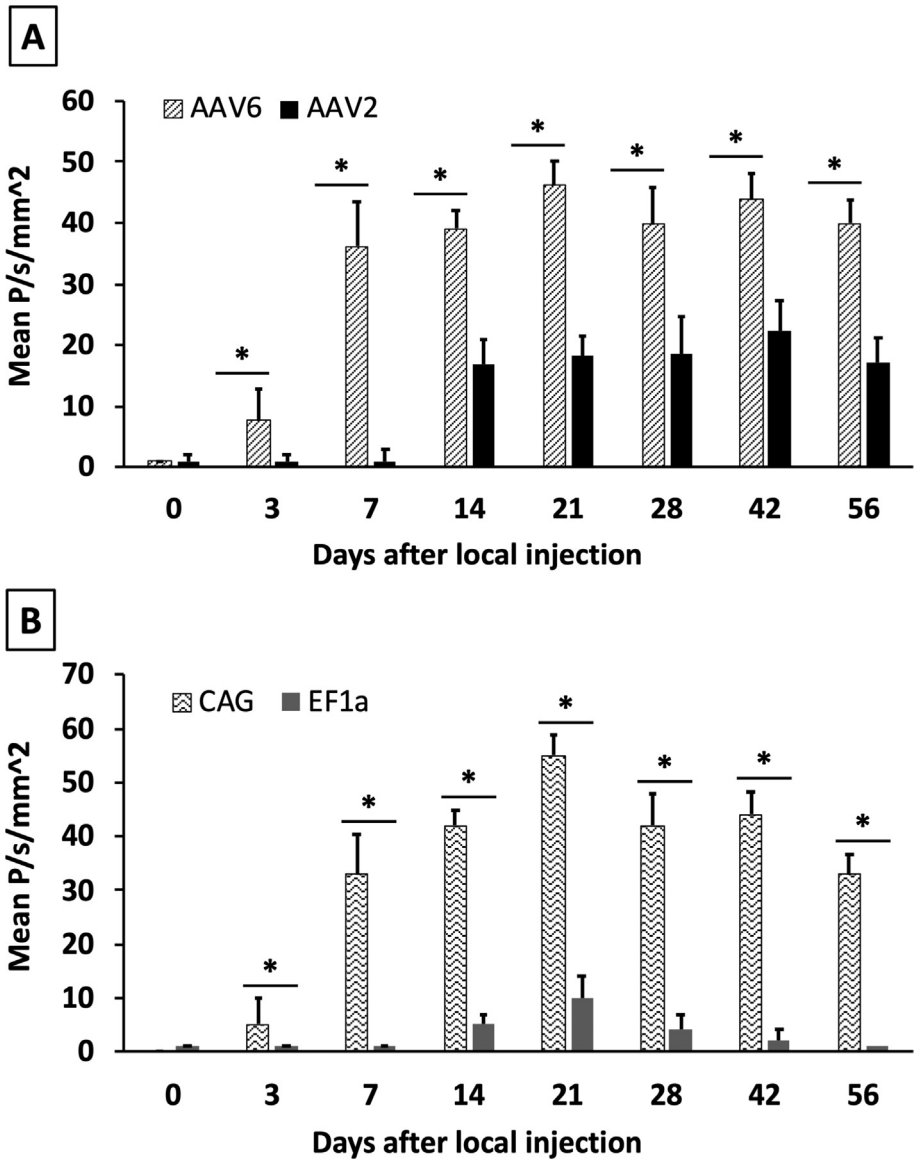

Figure 4 Comparison of AAV serotypes and gene promoters in NP cell transduction efficiency *in vivo*. Both AAV2 and AAV6 serotypes (3 μL, 10^{11} GC/mL) were injected into Co6/7 of C57Bl/6 mice and BLi was serially performed (**A**). AAV6 showed better transduction efficiency and kinetics compared to AAV2. Moreover, AAV6 hit near maximal BLi intensity 7 days following local injection into the NP and was able to maintain a similar amount of fLuc expression up to 56 days, while AAV2 took significantly at least twice as long to reach maximal intensity and mean peak intensity was also significantly less than what was achieved with AAV6. In separate experiments, both AAV6-CAG-fLuc and AAV6-EF1α-fLuc particles (3 μL, 10^{11} GC/mL) were injected into Co6/7 of C57Bl/6 mice and BLi was performed serially (**B**). While AAV-CAG worked well, the EF1α promoter provided very little BLi at all timepoints. Error bars show SEM. '*' represents statistical significance, $P < 0.05$. P = photon, s = seconds.

the human elongation factor-1α (EF1α) promoter and the CAG promoters have been found to direct varying amounts of transgene expression within AAV vectors both *in vitro*[46] and *in vivo*[47] depending on the context. Therefore, while AAV6-CAG constructs had been demonstrating good effectiveness in the NP *in vivo* thus far, we next wanted to determine whether another widely studied constitutive promoter for *in vivo* use, EF1α, would provide superior transduction efficiency or kinetics of transgene expression. Both AAV6-CAG-fLuc and AAV6-EF1α-fLuc particles (3 μL, 10^{11} GC/mL) were injected into caudal IVDs (Co6/7) of C57Bl/6 mice and longitudinal BLi was performed at 3, 7, 14, 21, 28, 35, 42, and 56 days to determine any differences. Interestingly, while the AAV-CAG combination continued to work very well *in vivo* with good reproducibility, the EF1α comparatively provided very little BLi at all timepoints (Fig. 4B). This was somewhat surprising given that the EF1α promoter has been shown to provide consistent expression *in vitro* and *in vivo* in a variety of cell types.[48—52] To be sure, a repeat experiment was conducted with a separate batch of AAV6-EF1α-fLuc, but similar results were found (data not shown). Therefore, AAV-EF1α may not be the best choice when designing experiments to drive transgene expression in NP cells *in vivo*.

Comparison of bioluminescence reporters

While fLuc was determined to perform well for BLi of NP cells *in vivo*, we next wanted to investigate whether other bioluminescence reporters may perform even better. One concern with fLuc in the IVD is that it requires an abundance of ATP for bioluminescence,[53] and since the NP is known to be relatively hypoxic and NP cells get most of their energy via anaerobic glycolysis,[54] we decided to also test another bioluminescence reporter, gLuc (*Gaussia* luciferase), that does not require ATP to achieve bioluminescence. In addition, GLuc is the smallest known luciferase (19kD) and its catalytic properties make it one of the "brightest" known luciferases,[55] so it was hypothesized that it might provide a stronger BLi signal when used *in vivo*.

We therefore injected either AAV6-CAG-fLuc or AAV6-CAG-gLuc (3 μL, 10^{11} GC/mL) into caudal IVDs (Co6/7) of C57Bl/6 mice and performed longitudinal BLi up to 56 days to determine the relative transduction efficiency and kinetics of transgene expression for each luciferase. While fLuc again provided consistently strong signal and favorable kinetics, we could not achieve any BLi signal with the use of gLuc in any of the animals tested (data not shown). To ensure that this lack of signal wasn't somehow due to the AAV serotype being used, we repeated this experiment two more times using both AAV2-CAG-gLuc and AAV3-CAG-gLuc. Again, we found no BLi signal at any of the timepoints tested (3—56 days, data not shown). This was true even with the use of two different substrates for the gLuc reporter: (1) the conventional substrate for gLuc, coelenterazine, and (2) a water-soluble version called coelenterazine-SOL (Nanolight Technology, Randolph, VT) that is less toxic and safer for repeated injections.[56] To make sure that we weren't missing the quick flash of bioluminescence inherent with gLuc, we also performed BLi in each of these conditions at varying timepoints after delivery of substrate: 30 sec, 1 min, 2 min, 4 min, 6 min, 8 min, and 10 min. Again, we found no bioluminescence at any of these timepoints. Due to the fact that we could not get gLuc to provide BLi under any of these conditions, we concluded that gLuc is not an appropriate bioluminescent reporter in NP cells *in vivo* and recommend that fLuc be used instead.

Off-target transgene expression

We next wanted to determine, in any of the conditions tested above using the fLuc reporter, if there were any signs of off-target transgene expression. In other words, even after local injection of each viral construct into the NP of a caudal IVD, did the virus migrate either through the cartilaginous endplate via diffusion or out of the annular puncture defect and cause expression of fLuc anywhere else in the body? This would be particularly important in studies using gene engineering *in vivo*, as these off-target effects could have unknown deleterious effects on the animals.

Upon review of the whole-body images of each mouse from all of the experiments described above (20 min after injection of luciferin), we did not find any evidence of off-target effects outside of the immediate area surrounding the injected Co6/7 IVD (data not shown). This held true even when larger injection volumes (5 μL) or titers (10^{13} GC/mL) were used. The farthest signal outside of each injected disc was found in the mice receiving the 5 μL injections (Fig. 2B), but again, that BLi was just slightly eccentric and felt to be due to mechanical disruption of the AF from the larger volume delivered. Using our described method, there was no evidence that any appreciable amount of AAV traveled anywhere else in the body via the systemic circulation (within the limits of our detection method). For achieving good transduction of NP cells *in vivo*, we therefore recommend injecting 3 μL of the AAV6 serotype at a titer of 10^{11} GC/mL, as it appears to be effective at achieving transgene expression without significant off-target effects.

Evaluation of transduction efficiency and toxicity *in vivo*

While BLi allows for the assessment of the kinetics of transgene expression over time and an approximation of transduction efficiency (based on the relative intensity of signal), we next wanted to more accurately quantify the exact number of murine NP cells successfully transduced *in vivo* following the local injection of AAV6 ± CPP into the disc. We therefore performed high-resolution 3D lightsheet microscopy of whole intact IVDs four weeks following local injection of 3 μL of AAV6-CAG-Cre (Cre recombinase), with or without the addition of a CPP, into caudal IVDs of mTmG mice (Co6/7). These mTmG mice were chosen because when the 'Cre' recombinase protein is expressed as part of the delivered transgene, it converts the baseline red fluorescent signal (tdTomato) in the cell membranes of these mice's cells to a green (EGFP, enhanced green fluorescent protein) color, thereby acting as a convenient indicator of successful viral transduction, transgene expression, and Cre recombination *in vivo*. Four weeks following injection, the mice were euthanized and their spines were carefully dissected and subjected to the PEGASOS method[42] of optically clearing tissue. Following optical tissue clearing of whole intact disc segments (the IVD with both adjacent vertebral bodies attached), these segments (Fig. 5A) were imaged three-dimensionally using a lightsheet microscope (Fig. 5B, C).

After 3D reconstruction of the imaging data, the number of successfully transduced NP cells were calculated using Imaris (Fig. 5D). It was found that 10^{11} GC/mL of AAV6 without the addition of CPP resulted in a mean transduction efficiency of only 2.3 ± 0.8%. With the addition of CPP, however, a titer of 10^{11} GC/mL achieved a mean transduction efficiency of 13.3 ± 1.8% ($P < 0.05$). Finally, when AAV6 was locally delivered at a higher titer of 6×10^{11} GC/mL, transduction efficiency significantly increased to 81.7 ± 9.8%. Lightsheet images of AAV6 alone and AAV + CPP are shown in Figure 5B and C, respectfully. Moreover, Figure S2 shows representative images of the 3D analysis (performed in Imaris) used to accurately determine exactly how many individual NP cells were successfully transduced and had transgene (Cre recombinase) expression.

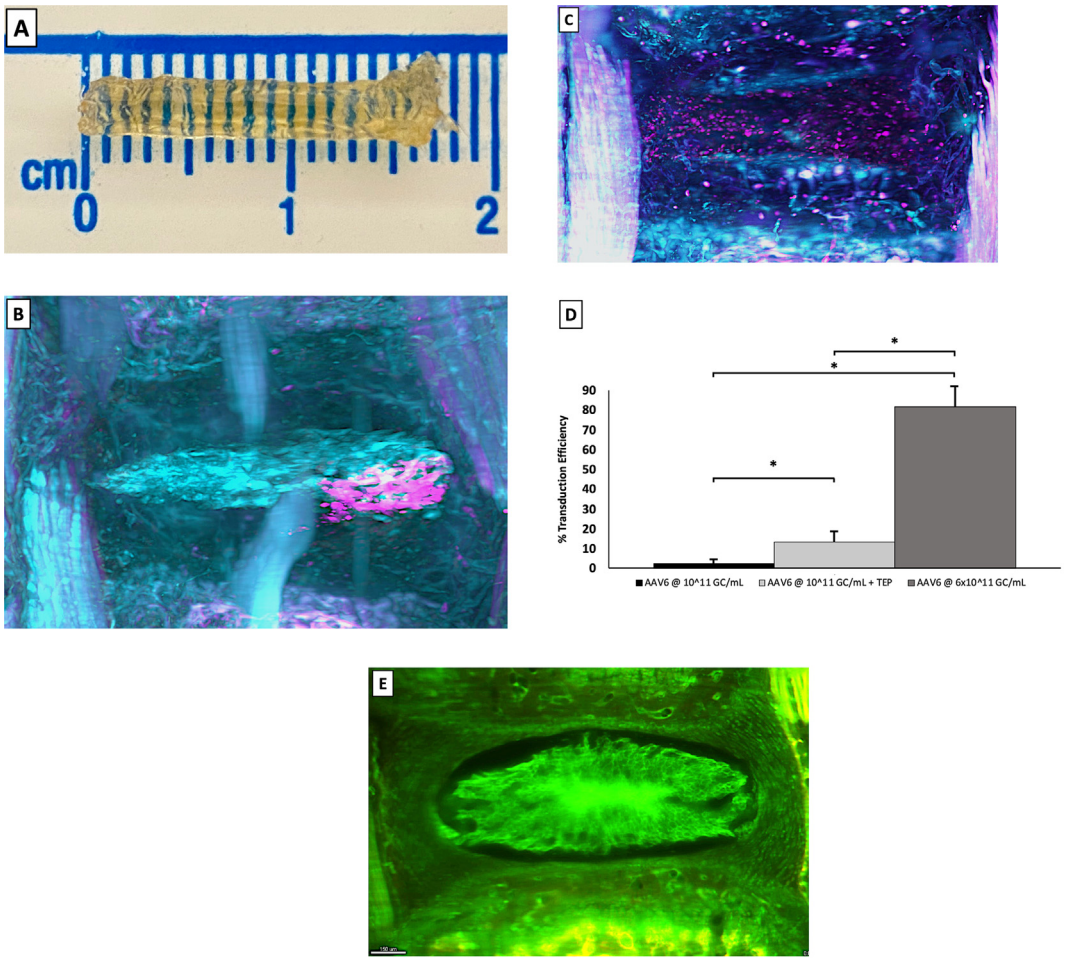

Figure 5 Assessment of NP cell transduction and whole IVD tissue architecture using 3D lightsheet microscopy. Caudal spines of mTmG mice were carefully dissected after euthanasia and then subjected to the PEGASOS method[42] of optically clearing whole intact tissue (**A**). These tails were then imaged using high-definition 3D lightsheet microscopy (**B, C**) and the number of successfully transduced NP cells were calculated for reach condition (**D**). The addition of CPP significantly increased the amount of NP cell transduction *in vivo*. In the 2D representative lightsheet images of the 3D dataset of AAV6 alone (B) and AAV6+CPP (C), the green/red fluorescence of mTmG mice have been changed to cyan/pink with pink representing cells that have been transduced and cyan cells having no transgene expression. Finally, a representative mid-sagittal two-dimensional picture of a non-punctured control IVD is shown (**E**). Compared to traditional histologic sections, a very accurate assessment of the cellular and tissue architecture can be achieved with this imaging method. Error bars show SEM. '*' represents statistical significance, $P < 0.05$.

Finally, because lightsheet microscopy allows fine details of the tissue structure to be assessed in intact, uninterrupted tissue three-dimensionally, we used it to assess for any signs of toxicity or pathologic cellular or tissue phenotypes following delivery of AAV6 ± CPP. To do this, we utilized a previously validated histologic grading system for IDD in mouse discs that takes into account five separate domains: (1) NP structure, (2) annulus fibrosus (AF) structure, (3,4) NP and AF clefts/fissures, and (5) the NP/AF boundary.[57] Overall, we found that 3D lightsheet microcopy could easily and accurately assign scores to each of these scoring domains from the histology-based grading system. As can be seen in Figure 5E, when turning off the software filters for fluorescence and looking at two-dimensional slices as opposed to 3D renderings (i.e., Fig. 5C, D), a very accurate assessment of the cellular and tissue architecture can be achieved with this imaging method. This is particularly true given the ability to scroll through each disc at ~2 μm intervals. Compared to a set of non-punctured controls (no AAV, $n = 3$), the discs that had AAV6 alone ($n = 5$) injected and the discs that had AAV6+CPP ($n = 5$) were scored independently by two experienced spine surgeons (CHK and SP). After thorough evaluation in 3D, there were no significant adverse effects on the cellular or tissue architecture of either the NP or AF following injection of AAV alone ($P = 0.09$) or AAV + CPP ($P = 0.06$). A summary of the grades is shown in Table S1.

Discussion

Recent advances in molecular biology have made the clinical application of gene therapy increasingly feasible and its potential to favorably alter the course of IDD is under

rigorous investigation. Gene transfer through the use of AAV vectors, either in a therapeutic attempt or in basic and translational research, is a fascinating and promising tool to manipulate both the complex physiology of NP cells and the IVD as a whole *in vivo*. To our knowledge, however, the ability of different AAV serotypes to transduce NP cells *in vivo*, and the experimental conditions to optimize transduction efficiency, have not been systematically compared. Herein, we assessed the transduction efficiency and kinetics of transgene expression in murine NP cells of caudal IVDs *in vivo* using the AAV-2 and -6 serotypes, injection volumes, viral titers, gene promoters, and bioluminescence reporters. Between these two serotypes, which are the serotypes that have been previously shown to have the highest tropism for NP cells *in vitro* compared to others,[41] AAV6 clearly performed best *in vivo* with respect to transduction efficiency, quick onset of transgene expression, and prolonged expression through 8 weeks. Moreover, we found that an injection volume of 3 μL and a titer 10^{11} GC/mL provided optimal transduction efficiency and kinetics while showing no appreciable off-target transgene expression. In addition, because no evidence of toxicity was found using high-definition 3D lightsheet imaging under these conditions, we recommend these parameters be considered for use in future studies using AAV vectors to transduce NP cells *in vivo*. Moreover, given the physical disruption of the AF in >80% of the animals receiving an injection volume of 5 μL, an injection volume of 3 μL is recommended for any injection of caudal murine discs in basic/translational studies, regardless of the application or goal.

In addition to finding these experimental parameters, which led to high transduction efficiency of NP cells *in vivo*, we found that a fLuc bioluminescent reporter works very well in NP cells *in vivo*. We have also defined, for the first time, the optimal window to perform BLi in mice after an intraperitoneal injection of d-luciferin. Interestingly, while the fLuc reporter worked well in the IVD, the gLuc reporter did not. Again, this was surprising given that gLuc is known to be much less dependent on ATP and the IVD heavily relies on anerobic metabolism. Therefore, when designing plasmids containing bioluminescent reporters for use in the IVD during the design phase of experiments, the fLuc reporter should be used in place of a gLuc reporter.

One important factor in determining the success of using viral-mediated gene therapy in NP cells of the IVD *in vivo* is the duration of transgene expression. In most gene transfer studies, there is a decline in transgene expression over time, and this can certainly be a significant limitation to effective gene therapy. Some evidence suggests that the duration of gene expression after adeno-associated viral transfer is limited because of an immune response to the injected virus.[18,58] This was not found to be the case up to 8 weeks, however. We hypothesize that this may be the case because the IVD is mostly avascular and encapsulated, conferring protection from the systemic immune system. This immune-privileged character of the disc may therefore serve to prevent immune reactivity, permit prolonged gene expression, and even protect the animal or patient from local or systemic illness resulting from injected AAV vectors.

We also showed for the first time that a CPP, in this instance the histidine-rich peptide LAH4, can be used to significantly increase AAV-mediated transduction efficiency of NP cells *in vivo* without any apparent toxicity or adverse effects on tissue or cellular architecture. CPPs, small polybasic peptides, are known to be able to penetrate cell membranes and have been used to deliver biologically active materials, including viruses,[59] into various cell types and tissues. CPPs show promise as an alternative strategy to chemical reagents that promote endosomal membrane disruption[60,61] because CPPs can promote the destabilization of the endosomal membrane upon acidification of the endosomal compartment without significant toxicity.[62] While only one CPP was tested in this study, LAH4, our promising results suggest that further study of CPPs in the IVD is warranted. In addition to LAH4, other CPPs should also be investigated as they may also further enhance transduction percentages or even allow for similar transduction efficiencies of NP cells at even lower viral titers. In addition to viral-based transduction methods, CPPs may aid in other gene engineering approaches in the IVD such as RNAi (RNA interference) or with the use of CRISPR (clustered regularly interspaced short palindromic repeats)-based technologies.

Finally, we investigated two novel applications of a relatively new and exciting technique called optical tissue clearing and 3D lightsheet microscopy. Herein, we applied this powerful technique to the IVD for the first time. First, it was used to aid in the accurate assessment of transduction efficiency *in vivo* (i.e., how many NP cells were successfully transduced compared to entire NP population). Secondly, the use of this imaging technique was explored as a potential complement to, or even novel replacement for, traditional two-dimensional histology in visualizing cell- and tissue-level architecture. As opposed to histologic sections, which are notoriously prone to sectioning artefact in the IVD due to the soft NP as well as limited to assessments in serial two-dimensional pictures, lightsheet microscopy allows for single-cell resolution of all cells in 3D in whole, intact tissue without the need for sectioning. Compared to histology, the 3D nature of the imaging dataset uniquely allows for the assessment of uninterrupted tissue structures such as collagen fibers, blood vessels, nerve fibers, etc. While it was not the primary focus of this paper, lightsheet microscopy may therefore be particularly well-suited to aid in the assessment of disc degeneration in a variety of basic and translational studies. We are therefore actively investigating this imaging technique following annular puncture and tail-looping models of disc degeneration while validating a grading system to assesses cellular and tissue architecture in three-dimensions.

Despite these encouraging results, several limitations of this study merit mention. First, the use of BLi provides only an indirect assessment of transduction efficiency, and therefore, many of the parameters studied herein, such as titer, volume, etc., were not assessed directly at an individual cellular level. That being said, the use of lightsheet microscopy with AAV6 confirms the BLi findings, including high levels of NP cell transduction *in vivo* without evidence of toxicity (including when CPPs were used). A second limitation is that only two AAV serotypes were tested. While other serotypes may provide further benefits in terms of higher transduction efficiencies, etc., the two serotypes tested were shown previously to be two of the serotypes

with some of the highest amounts of tropism for NP cells *in vitro*.[41] Of course it is possible that differences exist between the *in vitro* and *in vivo* environments, however. Similarly, there are many other gene promoters and bioluminescent reporters that could possibly outperform what was investigated here. Taken together, further studies systematically comparing other AAV serotypes, promoters, and reporters in this setting are warranted.

Conclusions

The IVD seems to be a superb site for AAV-mediated transfer of therapeutic genes, because the cells of the NP can be transduced efficiently, there is a low possibility of immune reaction, and longer-term gene expression is possible given the relatively quiescent character of NP cells. These findings presented herein will contribute to the success of using AAV6-mediated gene delivery in a variety of applications for basic and translational studies of the IVD, as well as potentially aid in the design of more efficient and effective gene therapeutic approaches for the treatment of IDD.

Author contributions

Study design: CHK, CO, HD, and SMP. Study conduct: CHK, CO, and SMP. Data collection: CHK and SMP. Data analysis: CHK and SMP. Data interpretation: CHK, HD, and SMP. Drafting manuscript: CHK and SMP. Approving final version of manuscript: CHK, CO, HD, and SMP. SMP takes responsibility for the integrity of the data analysis.

Conflict of interests

The authors have no financial conflicts of interest to disclose.

Acknowledgements

This work was supported by a Veteran Affairs Career Development Award (IK2-BX003845). We would also like to acknowledge Mesfin Teklemariam, PhD, for his help performing the animal experiments.

Appendix A. Supplementary data

Supplementary data to this article can be found online at https://doi.org/10.1016/j.gendis.2020.12.009.

References

1. Clark S, Horton R. Low back pain: a major global challenge. *Lancet*. 2018;391(10137):2302.
2. Wang C, Wang WJ, Yan YG, et al. MicroRNAs: new players in intervertebral disc degeneration. *Clin Chim Acta*. 2015;450:333—341.
3. Katz JN. Lumbar disc disorders and low-back pain: socioeconomic factors and consequences. *J Bone Joint Surg Am*. 2006;88(Suppl 2):21—24.
4. Han I, Ropper AE, Konya D, et al. Biological approaches to treating intervertebral disk degeneration: devising stem cell therapies. *Cell Transplant*. 2015;24(11):2197—2208.
5. Sampara P, Banala RR, Vemuri SK, Av GR, Gpv S. Understanding the molecular biology of intervertebral disc degeneration and potential gene therapy strategies for regeneration: a review. *Gene Ther*. 2018;25(2):67—82.
6. Kadow T, Sowa G, Vo N, Kang JD. Molecular basis of intervertebral disc degeneration and herniations: what are the important translational questions? *Clin Orthop Relat Res*. 2015;473(6):1903—1912.
7. Chen S, Luo M, Kou H, Shang G, Ji Y, Liu H. A review of gene therapy delivery systems for intervertebral disc degeneration. *Curr Pharm Biotechnol*. 2020;21(3):194—205.
8. Thompson JP, Oegema Jr TR, Bradford DS. Stimulation of mature canine intervertebral disc by growth factors. *Spine*. 1991;16(3):253—260.
9. Osada R, Ohshima H, Ishihara H, et al. Autocrine/paracrine mechanism of insulin-like growth factor-1 secretion, and the effect of insulin-like growth factor-1 on proteoglycan synthesis in bovine intervertebral discs. *J Orthop Res*. 1996;14(5):690—699.
10. Glansbeek HL, van Beuningen HM, Vitters EL, Morris EA, van der Kraan PM, van den Berg WB. Bone morphogenetic protein 2 stimulates articular cartilage proteoglycan synthesis in vivo but does not counteract interleukin-1alpha effects on proteoglycan synthesis and content. *Arthritis Rheum*. 1997;40(6):1020—1028.
11. Tim Yoon S, Su Kim K, Li J, et al. The effect of bone morphogenetic protein-2 on rat intervertebral disc cells in vitro. *Spine*. 2003;28(16):1773—1780.
12. Mern DS, Tschugg A, Hartmann S, Thome C. Self-complementary adeno-associated virus serotype 6 mediated knockdown of ADAMTS4 induces long-term and effective enhancement of aggrecan in degenerative human nucleus pulposus cells: a new therapeutic approach for intervertebral disc disorders. *PLoS One*. 2017;12(2):e0172181.
13. Wallach CJ, Sobajima S, Watanabe Y, et al. Gene transfer of the catabolic inhibitor TIMP-1 increases measured proteoglycans in cells from degenerated human intervertebral discs. *Spine*. 2003;28(20):2331—2337.
14. Robbins PD, Ghivizzani SC. Viral vectors for gene therapy. *Pharmacol Ther*. 1998;80(1):35—47.
15. Hacein-Bey-Abina S, Von Kalle C, Schmidt M, et al. LMO2-associated clonal T cell proliferation in two patients after gene therapy for SCID-X1. *Science*. 2003;302(5644):415—419.
16. Moon SH, Nishida K, Gilbertson LG, et al. Biologic response of human intervertebral disc cells to gene therapy cocktail. *Spine*. 2008;33(17):1850—1855.
17. Gilbertson L, Ahn SH, Teng PN, Studer RK, Niyibizi C, Kang JD. The effects of recombinant human bone morphogenetic protein-2, recombinant human bone morphogenetic protein-12, and adenoviral bone morphogenetic protein-12 on matrix synthesis in human annulus fibrosis and nucleus pulposus cells. *Spine J*. 2008;8(3):449—456.
18. Yang Y, Nunes FA, Berencsi K, Furth EE, Gönczöl E, Wilson JM. Cellular immunity to viral antigens limits E1-deleted adenoviruses for gene therapy. *Proc Natl Acad Sci U S A*. 1994;91(10):4407—4411.
19. Mazzolini G, Narvaiza I, Pérez-Diez A, et al. Genetic heterogeneity in the toxicity to systemic adenoviral gene transfer of interleukin-12. *Gene Ther*. 2001;8(4):259—267.
20. Nemunaitis J, Cunningham C, Buchanan A, et al. Intravenous infusion of a replication-selective adenovirus (ONYX-015) in cancer patients: safety, feasibility and biological activity. *Gene Ther*. 2001;8(10):746—759.
21. Lozier JN, Csako G, Mondoro TH, et al. Toxicity of a first-generation adenoviral vector in rhesus macaques. *Hum Gene Ther*. 2002;13(1):113—124.

22. Berns KI, Linden RM. The cryptic life style of adeno-associated virus. *Bioessays*. 1995;17(3):237—245.
23. Bainbridge JW, Smith AJ, Barker SS, et al. Effect of gene therapy on visual function in Leber's congenital amaurosis. *N Engl J Med*. 2008;358(21):2231—2239.
24. Cideciyan AV, Aleman TS, Boye SL, et al. Human gene therapy for RPE65 isomerase deficiency activates the retinoid cycle of vision but with slow rod kinetics. *Proc Natl Acad Sci U S A*. 2008;105(39):15112—15117.
25. Hauswirth WW, Aleman TS, Kaushal S, et al. Treatment of leber congenital amaurosis due to RPE65 mutations by ocular subretinal injection of adeno-associated virus gene vector: short-term results of a phase I trial. *Hum Gene Ther*. 2008;19(10):979—990.
26. Maguire AM, Simonelli F, Pierce EA, et al. Safety and efficacy of gene transfer for Leber's congenital amaurosis. *N Engl J Med*. 2008;358(21):2240—2248.
27. Nathwani AC, Tuddenham EG, Rangarajan S, et al. Adenovirus-associated virus vector-mediated gene transfer in hemophilia B. *N Engl J Med*. 2011;365(25):2357—2365.
28. Hwu WL, Muramatsu SI, Tseng SH, et al. Gene therapy for aromatic L-amino acid decarboxylase deficiency. *Sci Transl Med*. 2012;4(134):134ra161.
29. Gaudet D, Méthot J, Déry S, et al. Efficacy and long-term safety of alipogene tiparvovec (AAV1-LPLS447X) gene therapy for lipoprotein lipase deficiency: an open-label trial. *Gene Ther*. 2013;20(4):361—369.
30. MacLaren RE, Groppe M, Barnard AR, et al. Retinal gene therapy in patients with choroideremia: initial findings from a phase 1/2 clinical trial. *Lancet*. 2014;383(9923):1129—1137.
31. Feuer WJ, Schiffman JC, Davis JL, et al. Gene therapy for leber hereditary optic neuropathy: initial results. *Ophthalmology*. 2016;123(3):558—570.
32. Lattermann C, Oxner WM, Xiao X, et al. The adeno associated viral vector as a strategy for intradiscal gene transfer in immune competent and pre-exposed rabbits. *Spine*. 2005;30(5):497—504.
33. Grieger JC, Samulski RJ. Adeno-associated virus as a gene therapy vector: vector development, production and clinical applications. *Adv Biochem Eng Biotechnol*. 2005;99:119—145.
34. Samulski RJ, Zhu X, Xiao X, et al. Targeted integration of adeno-associated virus (AAV) into human chromosome 19. *EMBO J*. 1991;10(12):3941—3950.
35. Zhao Y, Jia Z, Huang S, et al. Age-related changes in nucleus pulposus mesenchymal stem cells: an in vitro study in rats. *Stem Cells Int*. 2017;2017:6761572.
36. Roberts S, Evans EH, Kletsas D, Jaffray DC, Eisenstein SM. Senescence in human intervertebral discs. *Eur Spine J*. 2006;15(Suppl 3):S312—S316.
37. Kim KW, Chung HN, Ha KY, Lee JS, Kim YY. Senescence mechanisms of nucleus pulposus chondrocytes in human intervertebral discs. *Spine J*. 2009;9(8):658—666.
38. Gruber HE, Ingram JA, Norton HJ, Hanley Jr EN. Senescence in cells of the aging and degenerating intervertebral disc: immunolocalization of senescence-associated beta-galactosidase in human and sand rat discs. *Spine*. 2007;32(3):321—327.
39. Srivastava A. In vivo tissue-tropism of adeno-associated viral vectors. *Curr Opin Virol*. 2016;21:75—80.
40. Zincarelli C, Soltys S, Rengo G, Rabinowitz JE. Analysis of AAV serotypes 1-9 mediated gene expression and tropism in mice after systemic injection. *Mol Ther*. 2008;16(6):1073—1080.
41. Mern DS, Thomé C. Identification and characterization of human nucleus pulposus cell specific serotypes of adeno-associated virus for gene therapeutic approaches of intervertebral disc disorders. *BMC Musculoskelet Disord*. 2015;16(1):341.
42. Liang H, Ma SY, Feng G, Shen FH, Joshua Li X. Therapeutic effects of adenovirus-mediated growth and differentiation factor-5 in a mice disc degeneration model induced by annulus needle puncture. *Spine J*. 2010;10(1):32—41.
43. Nguyen AT, Dow AC, Kupiec-Weglinski J, Busuttil RW, Lipshutz GS. Evaluation of gene promoters for liver expression by hydrodynamic gene transfer. *J Surg Res*. 2008;148(1):60—66.
44. Liu Y, Okada T, Nomoto T, et al. Promoter effects of adeno-associated viral vector for transgene expression in the cochlea in vivo. *Exp Mol Med*. 2007;39(2):170—175.
45. Damdindorj L, Karnan S, Ota A, et al. Assessment of the long-term transcriptional activity of a 550-bp-long human beta-actin promoter region. *Plasmid*. 2012;68(3):195—200.
46. Gopalkrishnan RV, Christiansen KA, Goldstein NI, DePinho RA, Fisher PB. Use of the human EF-1alpha promoter for expression can significantly increase success in establishing stable cell lines with consistent expression: a study using the tetracycline-inducible system in human cancer cells. *Nucleic Acids Res*. 1999;27(24):4775—4782.
47. Gill DR, Smyth SE, Goddard CA, et al. Increased persistence of lung gene expression using plasmids containing the ubiquitin C or elongation factor 1alpha promoter. *Gene Ther*. 2001;8(20):1539—1546.
48. Liew CG, Draper JS, Walsh J, Moore H, Andrews PW. Transient and stable transgene expression in human embryonic stem cells. *Stem Cell*. 2007;25(6):1521—1528.
49. Kosuga M, Enosawa S, Li XK, et al. Strong, long-term transgene expression in rat liver using chicken beta-actin promoter associated with cytomegalovirus immediate-early enhancer (CAG promoter). *Cell Transplant*. 2000;9(5):675—680.
50. Oba Y, Ojika M, Inouye S. Firefly luciferase is a bifunctional enzyme: ATP-dependent monooxygenase and a long chain fatty acyl-CoA synthetase. *FEBS Lett*. 2003;540(1—3):251—254.
51. Salvatierra JC, Yuan TY, Fernando H, et al. Difference in energy metabolism of annulus fibrosus and nucleus pulposus cells of the intervertebral disc. *Cell Mol Bioeng*. 2011;4(2):302—310.
52. Goerke AR, Loening AM, Gambhir SS, Swartz JR. Cell-free metabolic engineering promotes high-level production of bioactive Gaussia princeps luciferase. *Metab Eng*. 2008;10(3—4):187—200.
53. Morse D, Tannous BA. A water-soluble coelenterazine for sensitive in vivo imaging of coelenterate luciferases. *Mol Ther*. 2012;20(4):692—693.
54. Jing D, Zhang S, Luo W, et al. Tissue clearing of both hard and soft tissue organs with the PEGASOS method. *Cell Res*. 2018;28(8):803—818.
55. Tam V, Chan WCW, Leung VYL, et al. Histological and reference system for the analysis of mouse intervertebral disc. *J Orthop Res*. 2018;36(1):233—243.
56. Tripathy SK, Black HB, Goldwasser E, Leiden JM. Immune responses to transgene-encoded proteins limit the stability of gene expression after injection of replication-defective adenovirus vectors. *Nat Med*. 1996;2(5):545—550.
57. Gratton JP, Yu J, Griffith JW, et al. Cell-permeable peptides improve cellular uptake and therapeutic gene delivery of replication-deficient viruses in cells and in vivo. *Nat Med*. 2003;9(3):357—362.
58. Matsushita M, Noguchi H, Lu YF, et al. Photo-acceleration of protein release from endosome in the protein transduction system. *FEBS Lett*. 2004;572(1—3):221—226.
59. Wadia JS, Stan RV, Dowdy SF. Transducible TAT-HA fusogenic peptide enhances escape of TAT-fusion proteins after lipid raft macropinocytosis. *Nat Med*. 2004;10(3):310—315.
60. El-Sayed A, Futaki S, Harashima H. Delivery of macromolecules using arginine-rich cell-penetrating peptides: ways to overcome endosomal entrapment. *AAPS J*. 2009;11(1):13—22.
61. Rueden CT, Schindelin J, Hiner MC, et al. ImageJ2: ImageJ for the next generation of scientific image data. *BMC Bioinformatics*. 2017;18(1):529.
62. Fleiss JL. Measuring nominal scale agreement among many raters. *Psychol Bull*. 1971;76(5):378—382.